48th AIAA/ASME/SAE/ASEE Joint Propulsion Conference & Exhibit
30 July - 01 August 2012, Atlanta, Georgia

AIAA 2012-3762

Characteristics of a Supersonic Model Combustor with Two-Staged Injections of Supercritical Kerosene

Taichang Zhang[1], Yueming Yuan[2], Jianguo Li[3] and Xuejun Fan[4]
LHD, Institute of Mechanics, Chinese Academy of Sciences, Beijing, 100190, P. R. China

Staged fuel injection plays an important role in designing of a scramjet combustor with balanced performance of combustion efficiency, flame stability, engine unstart, heat release distribution and subsonic/supersonic combustion mode transition. In this paper, a Mach 2.5 model combustor with two-staged fuel injections has been tested in airflow of total temperatures of 1500 K and total pressures of 1.3 MP. Supercritical kerosene with temperature of about 760 K was injected through two integrated fuel injection/flame-holder cavity modules. The effects of fuel injection distribution (injector spacing and fuel ratio) on the combustion pressure rise, thrust increment, lean blowout limit, wall temperature distribution and engine "unstart" have been examined.

Nomenclature

C	=	cavity	I	=	injector
Ma	=	Mach number	P	=	pressure, MPa
Q	=	mass flowrate	$\Delta\Gamma$	=	specific thrust increment
T	=	temperature, K	Φ	=	equivalence ratio
ΔX	=	interval between first- and second-stage injectors	x	=	streamwise location from combustor entrance

Subscripts

0	=	*stagnant condition*	*1*	=	*first-stage*
2	=	*second-stage*	*f*	=	*fuel*
s	=	*static condition*	*w*	=	*wall*
inj	=	*injection*			

Keywords: staged injection, supercritical kerosene, flame stability, heat release distribution, supersonic combustion

[1] Assistant Professor, State Key Laboratory of High Temperature Gas Dynamics, taichang@imech.ac.cn, No. 15 Beisihuanxi Road, Beijing, China, Member AIAA.

[2] Assistant Professor, State Key Laboratory of High Temperature Gas Dynamics, Member AIAA.

[3] Professor, State Key Laboratory of High Temperature Gas Dynamics.

[4] Professor, State Key Laboratory of High Temperature Gas Dynamics, xfan@imech.ac.cn, No. 15 Beisihuanxi Road, Beijing, China, Member AIAA ..

I. Introduction

IN hydrocarbon-fueled scramjet operations, the onboard fuel will be also used as a coolant and its temperature and state will vary with different flight stages. When both fuel temperature and pressure are higher than the thermodynamic critical point, the fuel becomes supercritical. Our previous experimental investigation [1] demonstrated that the use of supercritical kerosene injection holds the potential of enhancing fuel-air mixing and promoting overall burning intensity. But further increase in the fuel flow rate and the pressure rise with single-stage injection was limited by the upstream propagation of boundary layer separation (resulting in engine "unstart") due to excessive heat release.[2]

The concept of staged fuel injection [3-7] utilizes dispersed heat release to avoid locally excessive pressure rise when using single-stage fuel injection at high equivalence ratios. As such, better pressure distributions and higher thrust can be attained in a staged supersonic combustor. [3-7] It is also advantageous to use proper fuel distributions to adjust the fuel delivery with different flight conditions and achieve optimized heat release distribution and engine performance. However, with staged fuel injection, the amount of fuel injected through each stage is reduced significantly, and might reach the lean blowout limit. [8] Therefore, it is a big challenge to realize highly efficient combustion, while at the meantime, to avoid flame blowout and engine unstart.

In present paper the characteristics of supersonic model combustors with two-staged injections of supercritical kerosene have been experimentally investigated. A Mach 2.5 model combustor with two-staged fuel injections has been tested in airflow of total temperatures of 1500 K and total pressures of 1.3 MP. Supercritical kerosene with temperature of about 760 K was injected through two integrated fuel injection/flame-holder cavity modules. Specifically, the study focused on effects of the staged fuel injection spacing and fuel flowrate ratio of the two stages on the combustion performance, flame stability, engine unstart and heat release distribution. The combustion performance was indicated by wall static pressure distribution and thrust increment. Flame stability was represented by the lean blowout limit. Heat release distribution is reflected by the measurement of wall temperature.

II. Experimental Setup and Operation

A. Direct-connect combustion

The experiments were conducted in a direct-connect wind tunnel facility, which consisted of a vitiated air supply system, a Ma 2.5 multi-purpose supersonic model combustor, and a fuel delivery and heating system. The vitiated air was supplied by combustion of H_2 in air with oxygen replenishment, which has the stagnation temperatures of 800-2100 K and the stagnation pressures of 0.6-4.0 MPa. The supersonic model combustor is shown in Fig. 1 (top). It has a total length of 1500 mm and consists of one nearly constant-area isolator of 400 mm and two divergent sections of 800 and 300mm with the expansion angles of 2.0 and 5.3 degrees, respectively. The entry cross section of the combustor is 50 mm in height and 70 mm in width. Two flame flame-holder cavity modules (C-1 and C-2) are installed on opponent sides of the combustor, each with a depth of 12 mm, a 45-degree aft ramp angle, and an overall length-to-depth ratio of 7. Among them, C-1 locates upstream the combustor, specifically with its leading edge at x = 628mm. Besides a cavity, C-2 comprises of seven identical blocks with a length of 50 mm and a width of 70 mm, as shown in Fig. 1 (bottom). The location of the cavity in the C-2 is changeable through different assemblage of the blocks and the cavity. Two orifices of 1.5 mm in diameter upstream of the first cavity C-1 are available for the pilot hydrogen injection. Two fuel injectors (I-1 and I-2) can be used. Each injector has two orifices of 2.8 mm in diameter. Specifically I-1 is located 56 mm upstream of the cavity C-1 and 48 mm upstream the pilot hydrogen, while I-2 is located 56 mm upstream of the cavity C-2. Distance A between two staged injectors is adjustable in the range of 40-390 mm through changing the location of the cavity in C-2. A 50 J/pulse spark plug (Xuzhou Combustion Control Technology Co. LTD, China) installed on one of the cavity floor was used for ignition.

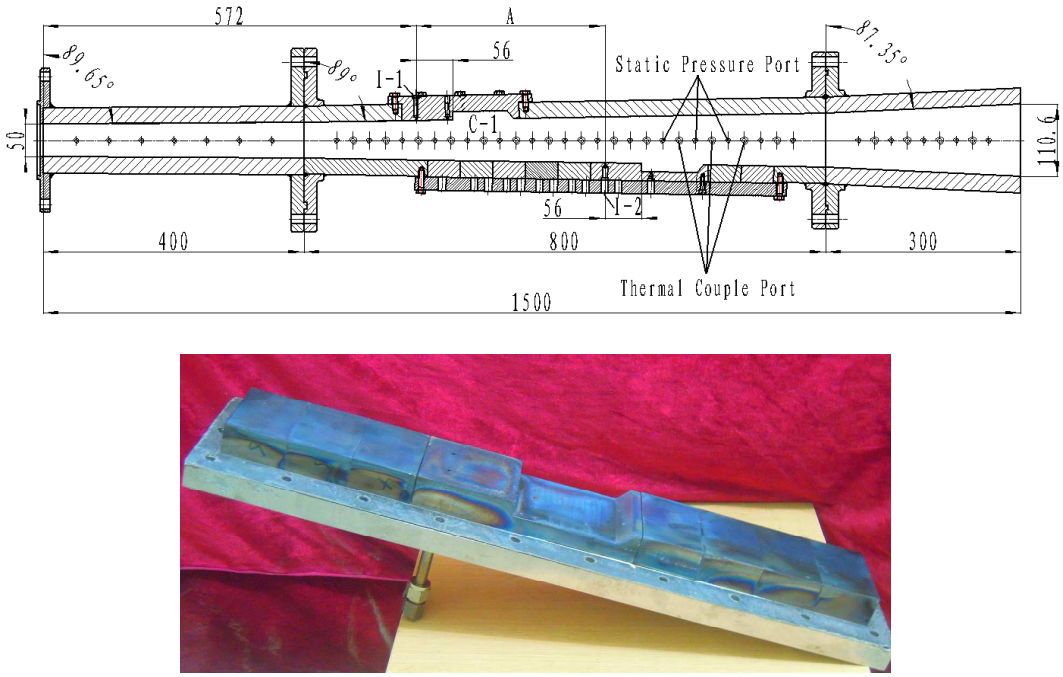

Figure 1. Schematic of the model combustor (top) and picture of a changeable integrated fuel injection/flameholder module (bottom). All length dimensions are in mm.

The two cavities were located at the opposite walls of the combustor, which ensured the full consumption of oxygen in the airflow and made the heat flux on the sidewall much more uniform.

Our recent experiments [8] indicated that it was easier to stabilize flame by injecting the fuel upstream of cavity than that from the floor of the cavity . Therefore, wall injection upstream of the cavity was used in this work.

B. Measurements system

The stagnation pressure and temperature of the vitiated air were respectively measured using a CYB-10S pressure transducer (accuracy ±0.1%, Beijing ZhongHangJiDian Technology Co. Ltd, China) and a Type-B thermocouple. Distributions of static pressure in the axial direction were determined using Motorola MPX2200 pressure transducers installed with 50 mm spacing along the centerline of the model combustor sidewalls. The static pressure distribution was used to not only calculate the thrust by a one-dimensional code, but also determine the lifted static pressure at the entrance of the combustor.

Wall temperature was measured using the K-type thermocouple (Diameter of xx) armored with a stainless steel sheath with 1.0 in diameter). The thermal couple was inserted into a hole in the combustor wall, as shown in Fig. 2. The tip of the armored thermal couple closely contacted with the bottom of the hole, which was 1.0 mm apart from the inner wall surface. The hole was filled with tin-lead solder. Thermocouples were installed from x = 475 mm to the exit with 50 mm spacing along the centerline of the model combustor sidewall. Although wall temperature will be redistributed due to tin-lead soldering, the relative variation of heat release along the combustor can be qualitatively reflected by the wall temperature measurement.

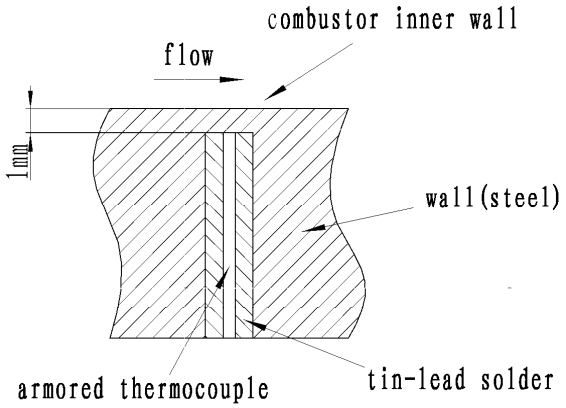

Fig. 2 Sketch of the wall temperature measurement

The entire test rig is mounted upright on a platform. Three weight sensors (Shanghai TM, Model No. NS-TH3), equilaterally spaced and connected in series, are used to support the platform and measure the thrust changes during the experiment. This system has a maximum force reading of 7500 N with a full scale uncertainty of 0.05%.

C. Kerosene delivery and heating system

Supercritical kerosene at temperature 760 ± 10 K and pressures of 3-6 MPa was prepared using a two-staged kerosene heating and delivering system.[9] A schematic of this system is shown in Fig. 2. The first stage was a storage heater that can heat kerosene of 0.8 kg up to 570 K with negligible coking deposits and the second stage was a continuous heater, which was capable of rapidly heating kerosene to 750 K within a few seconds.

Prior to each experiment, the kerosene in a storage cylinder was pumped into the first-stage heater by a piston driven by high-pressure nitrogen gas. Two pneumatic valves (Swagelok, Model No. SS6UM and SS10UM) installed, respectively, at the exits of the first- and second-stage heaters were employed to turn on/off the two heaters sequentially. When kerosene in the first-stage heater reached a desired temperature at a given pressure, it was pressed into the second-stage heater and heated up to the working temperature before injected into the model combustor. Two groups of K-type thermocouples (Omega, Model No. KMQSS-0.032E), denoted in Fig. 3, were installed on the surface of or inserted into the heater tubes. These thermocouples were used to monitor the fuel temperature distribution along the heating system and achieved the feedback control of the heating system. Steady fuel temperature and pressure at the exit of the heating system were accomplished and maintained during each experiment.

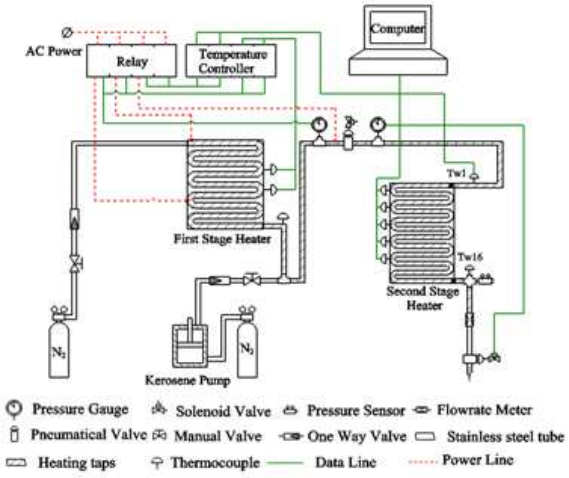

Fig. 3 Kerosene delivery and heating system

Mass flow rates of the supercritical kerosene were controlled and measured by using sonic nozzles. The associated calibration procedure has been documented in ref. The different size of the sonic nozzle was chosen according to the desired mass flow rate of the supercritical kerosene in the experiment. It was installed at the exit of the second-stage heater, as shown in Fig. 3. The mass flow rate of each sonic nozzle was determined on the base of the fuel temperature (T_f) and pressure (P_f) measured just upstream the nozzle. Considering the measurement accuracies of throat area, fuel pressure, and fuel temperature, the overall uncertainty associated with the measured fuel mass flow rate was within 5%. The pressure (P_{inj}) downstream the sonic nozzle was also measured and used as the injection pressure.

D. Experimental operation

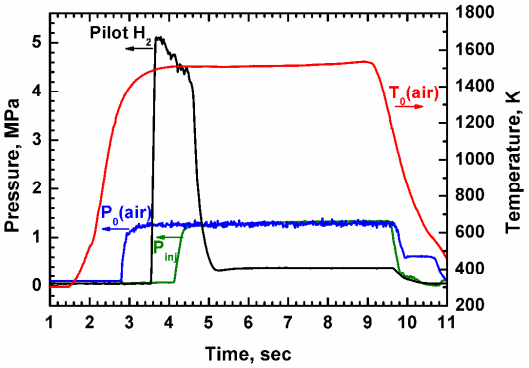

Fig. 4 Time histories of pilot gas pressure, supercritical kerosene pressure, stagnation temperature and pressure of the vitiated air during an experiment.

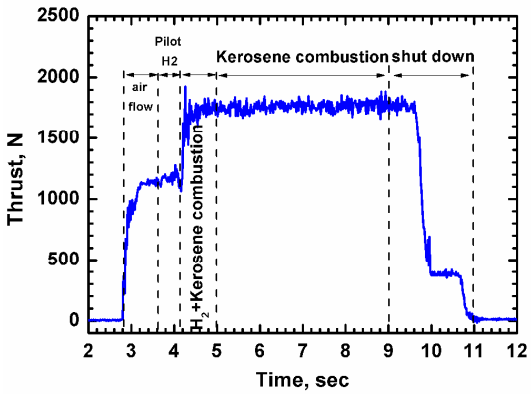

Fig. 5 Variation of thrust with time.

Figure 4 shows the typical time histories of pilot hydrogen pressure, supercritical kerosene pressure, total pressure and total temperature of the vitiated air during an experiment in a Ma = 2.5 supersonic flow. The vitiated air was started at 2.9 s, pilot hydrogen was injected at 3.6 s, and the supercritical kerosene was injected at 4.2 s. The pilot hydrogen was shut down completely at 5.0 s. The vitiated air and kerosene are shut down at 9.0 s and delay about 0.5 s due to the operation of the valve. Fig. 4 indicates that both the inlet airflow and kerosene flow are steady. The equivalence ratio of pilot hydrogen used in this work is about 0.08.

Figure 5 shows the typical variation of thrust with time in an experiment. Thrust in the time range of 2.9-3.6 s was produced by gas dynamic. The thrust at this condition can be regarded as reference thrust and should be subtracted from thrusts obtained with fuel injection and combustion to get the net thrust increment. The slight increment in 3.6-4.2 s was due to the combustion of pilot hydrogen. In 4.2-5.0 s kerosene was ignited and the combustion of kerosene and hydrogen produces the further thrust increment. Since pilot gas was completely shut down at 5.0 s, thrust in the time range of 5.0-9.0 s was produced by kerosene combustion and gas dynamic. Thrust curve shows some fluctuations during kerosene combustion, thus average of thrust in 6.0-9.0 s was used to obtain the thrust increment due to kerosene combustion. The specific thrust increment is defined as the thrust increment per unit of air mass flowrate.

III. Results and Discussions

In this section, effects of the spacing ΔX between two-staged fuel injectors on the static pressure distribution, thrust and wall temperature distribution were examined first. Subsequently, effects of the second stage injection on the flame stability were investigated at ΔX =190 and 390. Finally, effects of fuel flowrate ratio of the two stages on the static pressure distribution, thrust and wall temperature distribution were investigated at ΔX = 190. All experimental conditions are listed in Table 1.

A. Effects of injectors spacing

In this series of experiments, the first injector was fixed at x = 572 mm. Eight locations varying from x=612 mm with 50 mm increment were used for the second stage fuel injection. The amount of fuel with equivalence ratio of approximate 0.50 was used for each stage.

Figure 6 gives a typical history of the static pressure measured at x = 600 mm normalized by the stagnation air pressure, which shows large fluctuation during combustion. To avoid ambiguity average value of each static pressure port over 3.0 s was used in the following discussion.

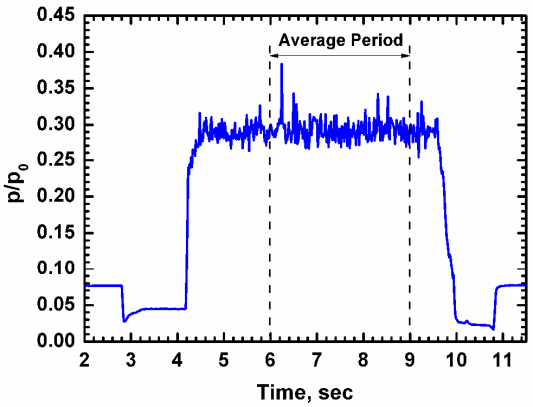

Fig. 6 Variation of normalized static pressure at x=600 mm with time.

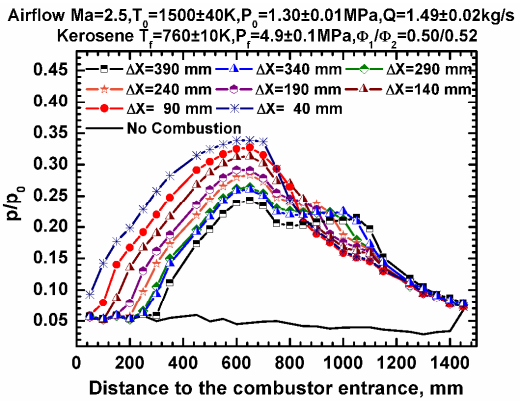

Fig. 7 Comparison of normalized static pressures with different spacings between injectors.

Figure 7 shows the comparison of normalized static pressure with fuel injections at different spacing ΔX. The pressure increases as the spacing decreases. Every time the spacing ΔX changes 50 mm the pressure curve will shift the same distance. At the largest injector spacing ΔX = 390 mm, two peaks in the static pressure can be clearly identified, which indicates the existence of two relatively independent reaction zones. As ΔX decreases, the second peak gradually disappears, which indicates the merging of two reaction zones and the interaction between them becomes stronger. The combustion of the upstream-injected fuel can provide an environment of large radical pool and high turbulent intensity for the downstream-injected fuel, thereby improving fuel/air mixing and enhancing burning processes. Note that in the case of X = 40 the static pressure at the entrance of the isolator was lifted as shown in the figure, which means the entry Mach number has been changed slightly and the combustor is called "unstart".

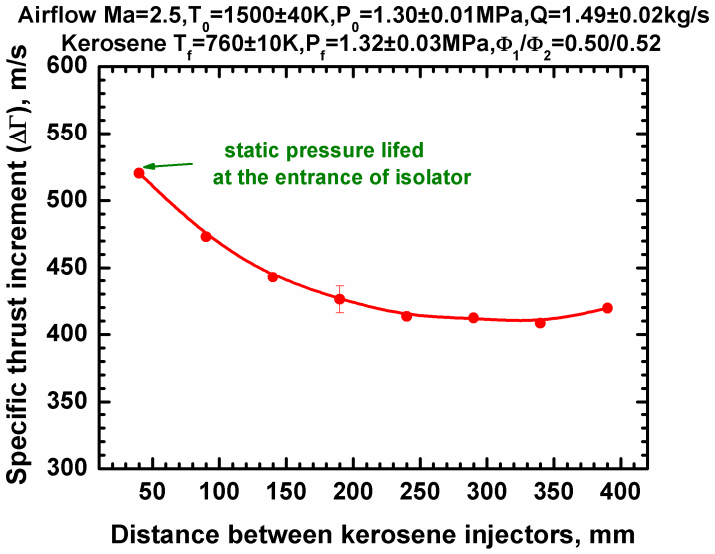

Fig. 8 Variation of specific thrust increments with different spacings between two stage injectors.

Figure 8 shows the variation of corresponding specific thrust increment. The specific thrust increments increase from 408 to 473 m/s when the spacing ΔX is reduced from 390 to 90 mm, with a plateau in the range of 240-390 mm and a steep rise at $\Delta X < 240$ mm. It can be concluded that the distributed injection becomes more effective with smaller streamwise interval between first- and second-stage injectors. Experiments with $\Delta X = 190$ were done for three times, which obtained 3% uncertainty. The uncertainty mainly attributed to the measurement accuracies of fuel flowrate, air flowrate, air pressure. Note that the reference thrust was overestimated, resulted from the separation at the combustor exit increased the thrust in the condition of no combustion. Thus the specific thrust increments were underestimated. The specific thrust increment was also calculated on the basis of the measured combustion static pressure distribution by a one-dimensional code without considering the friction. The calculated values were about 30% higher than experimental results.

The wall temperature distributions were also measured for these experiments. Figure 9 shows the distributions at different moments when the spacing ΔX was 240 mm. The equivalence ratio of pilot hydrogen was about 0.08 and its run time is about 1.0 s. Compared with the equivalence ratio and run time of kerosene, the contribution of hydrogen combustion to the wall temperature can be neglected. The figure shows the distributions at 0 and 4 seconds are identical. There is only slight increase until 6.0 s. The outlines of wall temperature distribution are similar in the period of 6.0-9.0 s: a peak around upstream cavity and a spike around x =1070 mm. The difference is that the peak slightly shifts downstream.

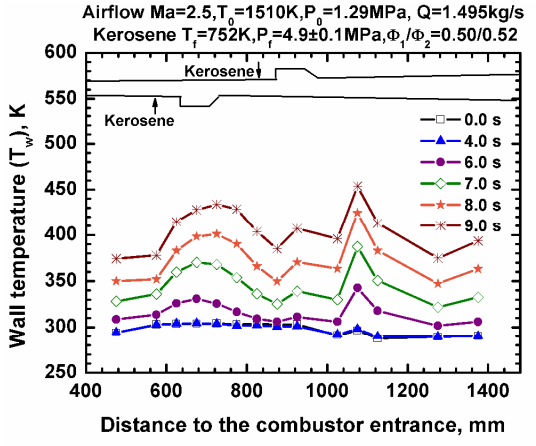

Fig. 9 Wall temperature distributions at different time with ΔX=240 mm.

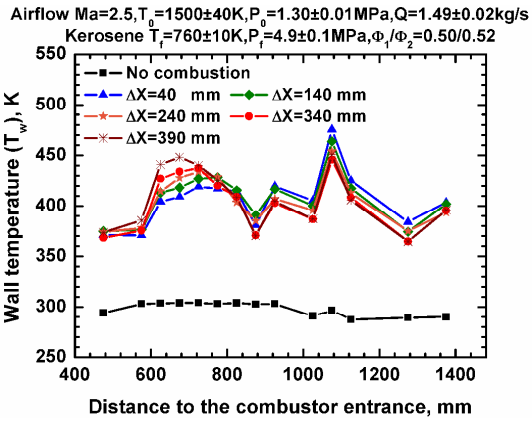

Fig. 10 Wall temperature distributions with different spacings between injectors at 9.0 s.

Figure 10 shows wall temperature distributions at 9.0 s with different spacings between two-staged injectors. When the spacing ΔX decreases, it can be seen that at $x < 900$ mm the wall temperatures reduce and the temperature peaks shift downstream, while temperatures rise at $x > 900$ mm. The temperature peaks present around $x = 700$ mm and $x = 1070$ mm, responding rear edge of the upstream cavity and downstream of the second-stage cavity. The optimal spacing is also about 130 mm in terms of temperature uniformity.

B. Effect of staged injection on the flame stability

As mentioned before, the second-stage injection should influence the flame of the first-stage injection in some degree. In this work, the influence of the second-stage injection on the flame stability was studied.

The criterion for flame stability is illuminated by Fig. 11. The figure shows the typical time histories of the pilot hydrogen pressure and the static combustion pressure at the location of x = 800 mm for three cases of stable combustion, blowout, and marginal state. Stable combustion is established if the combustion pressure maintained at least 4.0 s after pilot hydrogen is turned off; flame blowout occurs immediately once the pilot hydrogen shut down. Marginal state is the case that the stable combustion stopped at an intermediate moment as shown in Fig. 11.

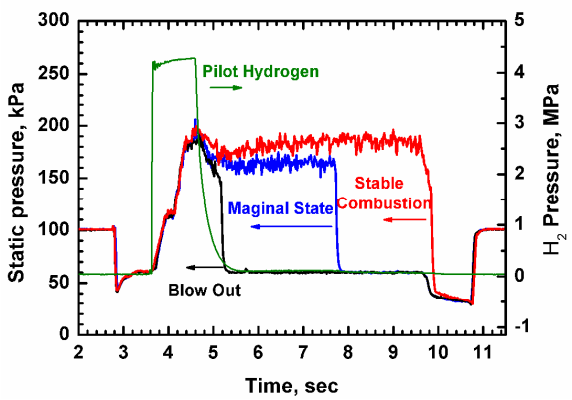

Fig. 11 Histories of pilot hydrogen pressure and static combustion pressure at x = 800 mm for the cases of stable combustion, blowout and marginal state.

Figures 12 and 13 show the detected lean blowout limit of supercritical kerosene in Ma=2.5 airflow at two typical spacings 190 and 390 mm. The total pressure and total temperature of airflow were 1.29±0.02 MPa and 1500±40 K. The air flowrates were 1.485±0.01 kg/s. The equivalence ratios of both the first- and second-stage injection were changed. Figure 12 shows that the lean blowout limit of first-stage injected fuel can be decreased by $\Phi_1 = 0.16$ from 0.26, once equivalence ratio of the second-stage injected fuel (Φ_2) is larger than 0.17. Since Φ_2 is hardly less than 0.20 in application, the influence of lower Φ_2 was not examined. Similarly, Fig. 13 shows that expansion of the lean blowout limit of first-stage injected fuel can be decreased by $\Phi_1 = 0.21$ from 0.26, when Φ_2 is larger than 0.20. Comparison of Figures 12 and 13 indicates the influence of the second-stage injection on the flame stability is reduced as the spacing ΔX increases. It can be concluded that the influence of the second-stage injection on the flame of first-stage injection is obvious for supercritical kerosene, which is totally different with the result for the hydrogen reported by Kirstein and coworkers[10]. The reason should be related with their mixing and combustion characteristics.

The combustion of second-stage injected fuel decrease the local velocity and increase the pressure in the combustor, which is beneficial for the flame stabilization. The mechanism for the effect of second-stage injection should be like mechanical or gasdynamic throttling, which has been proved to enhance the ignition and flame stabilization[11].

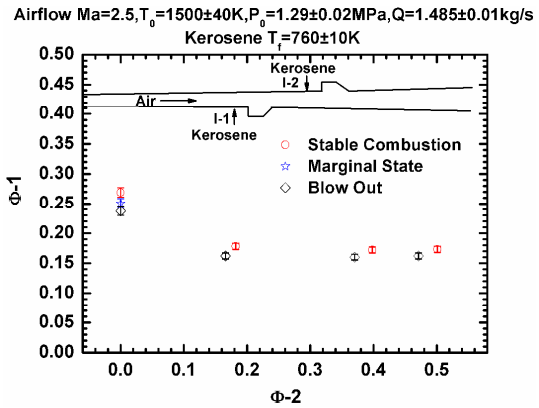

Fig. 12 Detection of fuel lean blowout limit with ΔX = 190 mm.

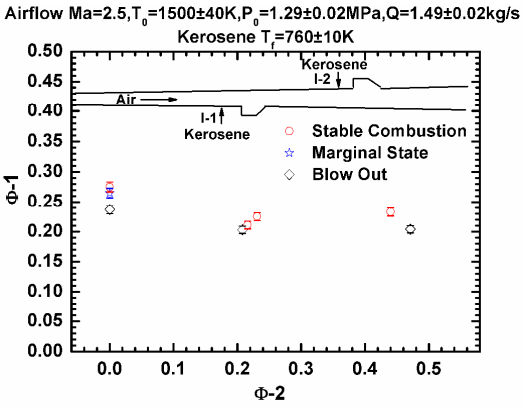

Fig. 13 Detection of fuel lean blowout limit with ΔX = 390 mm.

C. Effect of fuel flowrate ratio of the two stages

Equal fuel flowrate of the two stages was used in above experiments. In this section the effect of fuel flowrate ratio of the two stages on the static pressure distribution, specific thrust increment and wall temperature distribution were examined. The spacing ΔX = 190 mm was fixed. Experiments were conducted in Ma 2.5 airflows with the total pressure 1.28±0.02

MPa and total temperature 1500±40 K. The air flowrates were 1.48±0.02 kg/s. The detail experimental conditions were included in Table 1.

First, the overall equivalence ratio was fixed 1.0, and the ratio was changed. Figure 14 shows the comparison of normalized static pressures at three equivalence ratio combinations. The bar in the figure denotes the extent of static pressure fluctuation. It can be seen that the pressures fluctuate apparently before the second stage injector while those after the second stage injector almost do not. It seems that the flame front moves forward and backward. The figure shows the static pressure with Φ_1=0.504/Φ_2=0.527 is similar to that with Φ_1=0. 636/Φ_2=0.360, and both higher than that with Φ_1=0.363/Φ_2=0.640. The specific thrust increment listed in Table 1 has the same trend.

Figure 15 shows the comparison of wall temperature distributions at 9.0 s for these experiments. It can be seen that the distributions are basically same.

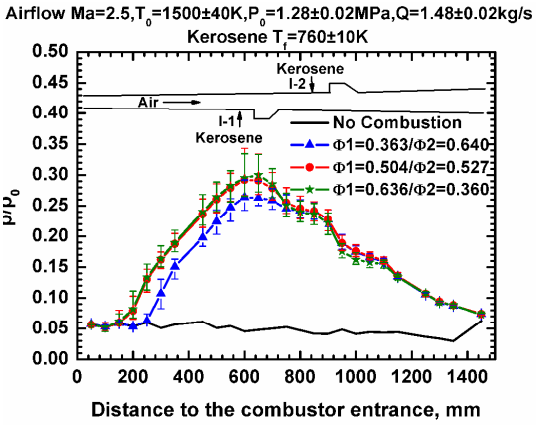

Fig. 14 Comparison of normalized static pressures at different ratios of Φ_1/Φ_2 (overall equivalence ratio of about 1.0)

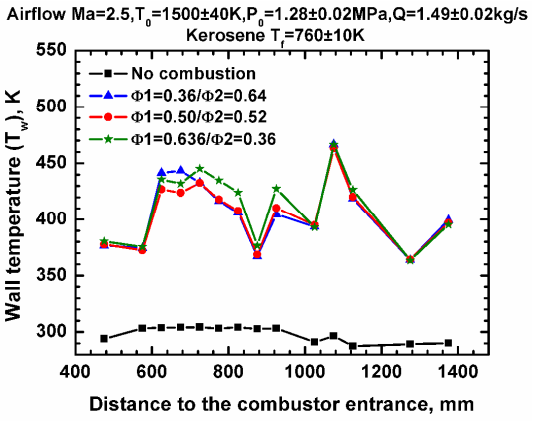

Fig. 15 Comparison of wall temperatures at the conditions same to figure 14.

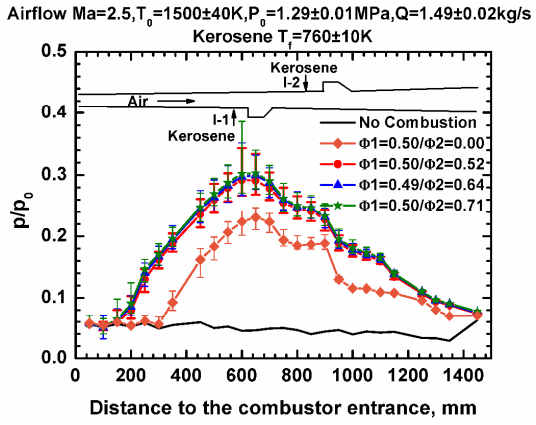

Fig. 16 Comparison of normalized static pressures with different Φ_2 (Φ_1=0.5).

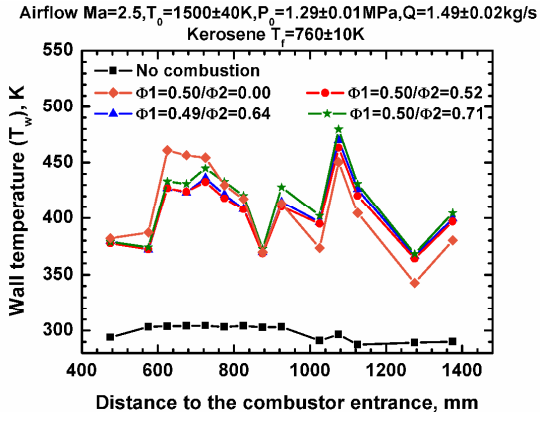

Fig. 17 Comparison of wall temperature distributions at the conditions same to Fig. 16.

Equivalence ratio of the first-stage injection was fixed at 0.50, and Φ_2 was changed. Figure 16 shows the comparison of normalized static pressures. Compared with Φ_2 = 0, the second-stage injection renders the pressure rise. When Φ_2 is larger than 0.50, the static pressure becomes identical, and all the specific thrust increments are about 425 m/s. Figure 17 shows their wall temperature distributions. Compared with Φ_2 = 0, it is interesting that the second-stage injection renders the

distribution more uniform.

It can be concluded that when the overall equivalence ratio is equal to or larger than 1.0, the specific thrust increment would be reduced at $\Phi_1 < 0.5$, while it is not effected at $\Phi_2 < 0.5$.

Table 1 Experimental conditions, specific thrust increments and flame stability

Figure	Vitiated air			Kerosene				ΔX,	$\Delta\Gamma$, m/s		Flame
	P_0, MPa	T_0, K	Q, g/s	P_f, MPa	P_{inj}, MPa	T_f, K	Φ_1/Φ_2	mm	Exp.	Cal.	stability
7-10	1.30	1493	1,509	4.88	1.30	757	0.49/0.51	40	520	629	
	1.30	1507	1,501	4.88	1.30	760	0.49/0.51	90	473	606	
	1.30	1494	1,509	4.88	1.30	756	0.50/0.52	140	443	592	
	1.26	1485	1,464	4.98	1.35	754	0.51/0.53	190	415	565	
	1.30	1509	1,500	5.00	1.35	757	0.504/0.527	190	423	570	
	1.29	1482	1,499	4.89	1.30	756	0.50/0.52	190	440	590	
	1.30	1509	1,495	4.89	1.30	751	0.50/0.52	240	413	564	
	1.30	1541	1,484	4.87	1.30	752	0.50/0.52	290	412	550	
	1.30	1501	1,506	4.89	1.30	756	0.49/0.51	340	408	552	
	1.31	1503	1,516	4.89	1.33	753	0.49/0.51	390	419	533	
11	1.28	1507	1,478	4.77	1.18	760	0.269/0.0	190			Stable
	1.28	1512	1,475	4.44	1.06	758	0.251/0.0	190			Marginal
	1.28	1495	1,484	4.19	0.99	755	0.237/0.0	190			Blowout
12	1.29	1508	1,488	4.62	0.67	758	0.16/0.37	190			Blowout
	1.27	1468	1,481	4.91	0.73	760	0.172/0.398	190			Stable
	1.27	1462	1,489	3.18	0.69	760	0.178/0.182	190			Stable
	1.29	1514	1,485	2.88	0.63	756	0.162/0.166	190			Blowout
	1.28	1483	1,489	4.60	0.66	763	0.162/0.471	190			Blowout
	1.27	1490	1,475	4.44	0.73	758	0.173/0.501	190			Stable
13	1.30	1495	1,507	4.29	1.03	755	0.237/0.0	390			Blowout
	1.28	1484	1,485	4.72	1.16	761	0.265/0.0	390			Marginal
	1.29	1514	1.490	4.85	1.22	756	0.275/0.0	390			Stable
	1.30	1551	1,478	3.75	0.86	759	0.211/0.216	390			Stable
	1.30	1541	1,483	4.03	0.93	763	0.225/0.231	390			Stable
	1.30	1531	1,495	3.59	0.82	754	0.203/0.208	390			Blowout
	1.28	1489	1,487	5.83	0.94	759	0.204/0.471	390			Blowout
	1.29	1535	1,475	4.12	0.94	759	0.233/0.44	390			Stable
14-15	1.27	1482	1,478	4.44	1.42	755	0.363/0.64	190	350	529	
	1.26	1485	1,464	5.00	1.35	754	0.51/0.53	190	415	565	
	1.30	1511	1,499	4.47	1.70	755	0.636/0.36	190	404	567	
16-17	1.30	1509	1,500	5.00	1.35	757	0.504/0.527	190	423	570	
	1.29	1478	1,504	4.67	1.44	755	0.493/0.636	190	422	576	
	1.29	1477	1,504	4.76	1.46	755	0.502/0.709	190	428	583	
	1.29	1528	1,477	6.17	2.23	759	0.50/0.0	190	283	439	

IV. Concluding Remarks

Two-staged fuel injection was introduced in this work to enhance the overall performance of a model supersonic combustor in terms of thrust, flame stability, combustion heat release distribution. The experiments were conducted using the direct-connect test facility at Institute of Mechanics, Chinese Academy of Sciences. The experiments were performed in Ma 2.5 airflows with total temperatures of 1500±40 K and total pressures of 1.29±0.03 MPa.

First, effects of the injector spacing on the static pressure distribution, specific thrust increment, impulse and wall temperature distribution were examined. The results showed that the distributed injection become more effective with a smaller streamwise injector spacing. The heat release distribution was analyzed by the measurement of wall temperature. The general feature of the wall temperature distribution included that a peak at rear edge of upstream cavity and a spike downstream of the second stage.

Effects of the second-stage injection on the flame stability were investigated. The lean blowout limit of fuel injected at first stage can be apparently expanded to lower equivalence ratios with the fuel injection from the second stage. The reducing of the spacing will help the flame stabilization at the first stage.

Effects of fuel flowrate ratio of the two stages on the static pressure distribution, specific thrust increment and wall temperature distribution were examined. When the overall equivalence ratio was equal to or larger than 1.0, the specific thrust increment would be reduced at $\Phi_1 < 0.5$, while it was not influenced at $\Phi_2 < 0.5$. Once spacing was fixed, variation of the ratio Φ_1/Φ_2 in a range of 0.5-2.0 slightly influenced the wall temperature distribution.

In summary, staged fuel injection is a powerful technique to balance the combustion performance, flame stability, heat release distribution, engine "unstart". Further work is needed to optimize the combustor design.

Acknowledgments

Current research program at the Chinese Academy of Sciences was supported by the National Natural Science Foundation of China under Contract No. 91016005 and 10621202. The authors would like to acknowledge Prof. G. Yu, Mr. X. S. Wei, Prof. X. N. Lu, Mr. L. J. Meng and Mr. Y. Li for their technical support.

References

1 Fan, X. J., Yu, G., Li, J. G., Zhang, X. Y.andSung, C. J., "Investigation of Vaperized Kerosene Injection and Combustion in a Supersonic Model Combustor," *Journal of Propulsion and Power,* Vol. 22, No. 1, 2006, pp.103-110.

2 Billig, F. S., Dugger, G. L.andWaltrap, P. J., "Inlet-combustor Interface Problem in Scramjet Engines," *Proceeding of the International Symposium on Air Breathing Engines,* Vol. 1972.

3 Billig, F. S., "Combustion Process in Supersonic Flow," *Journal of Propulsion and Power,* Vol. 4, No. 3, 1988, pp.209-216.

4 Thomas, S. R.andGuy, R. W., "Scramjet Testing from Mach 4-20 Present Capability and Needs for the Ninties," 1990, pp.AIAA Paper 90-1388.

5 Tomioka, S., Murakami, A., Kudo, K.andMitani, T., "Combustion Tests of a Staged Supersoinc Combustor with a Strut," *Journal of Propulsion and Power,* Vol. 17, No. No. 2, 2001, pp.293-300.

6 Tomioka, S., Kobayashi, K., Kudo, K., Murakami, A.andMitani, T., "Effects of Injection Configuration on Performance of a Staged Supersonic Combustor," *Journal of Propulsion and Power,* Vol. 19, No. No. 5, 2003, pp.876-884.

7 Fan, X. J., Yu, G., Li, J. G., Lu, X. Y.andSung, C. J., "Performance of Supersonic Model Combustors with Distributed Injection of Supercritical Kerosene," Forty-Third AIAA/ASME/SAE/ASEE Joint Propulsion

Conference, 2007, pp.AIAA Paper No. 2007-5406.

8 Wang, J., Fan, X. J., Zhang, T. C., Yu, GandLi, J. G., "Measurements of the Blowout Limits of Supercritical Aviation Kerosene in a Supersonic Combustor," 47th AIAA Joint Propulsion Conference, 2011, pp.2011-6108.

9 Fan, X. J., Zhong, F. Q., Yu, G., Li, J. GandSung, C. J., "Catalytic Cracking and Heat Sink Capacity of Aviation Kerosene Under Supercritical Conditions," *Journal of Propulsion and Power,* Vol. 25, No. 6, 2009, pp.1226-1232.

10 Kirstein, S., Maier, D., Fuhrmann, T., Hupfer, A.andKau, H., "Experimenal Study on Staged Injection in a Supersonic Combustor," *16th AIAA/DLR/DGLR International Space Planes and Hypersonic Systems and Technologies Conference,* Vol. 2009, pp.AIAA 2009-7343.

11 Li, J. G., Ma, F. H., Yang, V., Lin, K.-C.andJackson, T. A., "A Comprehensive Study of Ignition Transient in an Ethylene-fueled Scramjet Combustor," 43th AIAA/ASME/SAE/ASEE Joint Propulsion Conference & Exhibit, 8-11 July 2007, pp.AIAA 2007-5025.